Experimental Thermographic Analysis of Thermal Effects Induced on a Human Head Exposed to 900-MHz Fields of Mobile Phones

Maria Daria Taurisano and André Vander Vorst, *Fellow, IEEE*

***Abstract*—This paper summarizes the results of an experimental research of thermal effects induced by electromagnetic exposure to wireless mobile communication equipment. A series of experiments has been performed in order to examine the time evolution of the temperature of some body-part surfaces exposed to electromagnetic radiation emitted by global system for mobile communication mobile phones (900 MHz). Special attention has been paid to the analysis of the human head, as this is the human part mainly exposed in normal conditions of mobile phone use.**

***Index Terms*—Infrared thermography, mobile communications, nonionizing radiation, temperature, thermal effects, risk analysis.**

I. Introduction

THE extraordinary worldwide growth of wireless communications and the consequent increase of users' exposure to microwaves have induced increasing concerns about possible health effects from the public opinion, media, electronic industry, health organizations, and scientific community [1], [2]. Mobile global system for mobile communication (GSM) cellular phones have often been identified as potential sources of health effects. The electromagnetic fields (EMFs) at 900 MHz are known to penetrate exposed tissues and induce energy absorption and, although mobile telephone handsets transmit low power (2-W maximum), the user's body absorbs power from the handset antenna. The head of the user is submitted to the highest localized RF exposure.

It is well known that absorbed microwave energy is converted into heat within biological tissues and that thermal effects depend on the SAR spatial distribution [3], [4], but, in most cases, the distribution and relative magnitude of this energy absorption and heating are not as well defined. A comprehensive database is available on effects of thermal nature, but it mainly concerns animal studies and *in vitro* studies. Considerable effort has been spent in modeling microwave absorption, but very little systematic experimental work has been done to measure the actual temperature within the human body. On the other hand, several methods of biological effects determination are based on thermal measurements [5], which are: 1) *calorimetric methods*, particularly suited for *in vitro* measurements, in which heating and cooling data can be analyzed to estimate the energy absorbed by an irradiated sample; 2) *thermometric methods*, used to measure the temperature due to microwaves with particular types of nonperturbing thermometer, but only a few ones are commercially available; and 3) thermographic techniques used to measure the temperature with particular thermographic cameras. This last technique is probably one of the most attractive and not yet in sufficient use. The originality of the research described in this paper is primarily in the use of thermography to measure human thermal effects, and quite a number of experimental data have been recorded [6], [7].

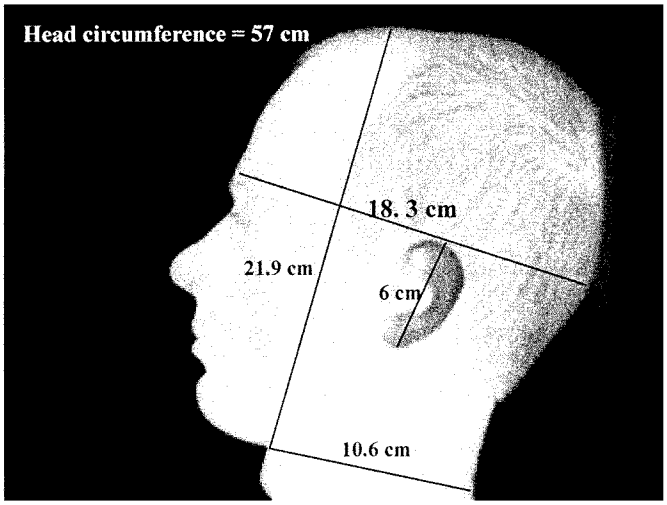

Fig. 1. Head main sizes.

II. Thermography

Thermographic cameras can be used to observe thermal distributions over a surface and obtain quantitative thermometric data. The use of thermographic cameras has been pioneered by the defense industry. In the last years, however, IR imaging has been developed for nonmilitary purposes, such as testing of materials evaluation of industrial processes and medical diagnoses [8]. For example, the use of IR emission from the human body has been developed for medical use and more effective methodologies are now being developed using the thermal behavior as a clinical tool [9]. However, while advanced computerized IR technology is evolving, thermography often remains only an occasional tool, not sufficiently used by the scientific community. Concerning bioelectromagnetics, IR thermography techniques for determining temperature and specific absorption rate (SAR) in models of biological bodies and animal cadavers exposed to strong EMFs were first developed by Guy [10] and have gained wide acceptance [11].

Manuscript received November 4, 1999; revised May 3, 2000.

The authors are with the Microwaves Department, Université catholique de Louvain, B-1348 Louvain-la-Neuve, Belgium.

Publisher Item Identifier S 0018-9480(00)09692-7.

TABLE I
HEAD AREAS DEFINITION AND SIZES

Area nr.	Subject	Area shape	Definition	Dimensions	Surface 2D (projection)
AR01	Ear	Round	Diameter along ear length	3 cm radius	28 cm^2
AR02	Cheek	Quadrilateral	Eye-nose base-chin base-ear base	10.5 lower base 6 cm height 4 cm upper base	43.5 cm^2
AR03	Frontal-temporal area	Quadrilateral	Frontal hair limit-frontal eyebrow Limit-occipital-parietal	18 lower base 6 cm height 15 cm upper base	99 cm^2
AR04	Neck	Quadrilateral	Ear base-chin base-nape-ear back	8.5 cm lower base 9 cm height 6 cm upper base	65 cm^2

In the research reported here, a series of experiments have been performed, in view of measuring the surface temperature of the human body during various phases of common GSM use. The focus has been put on how the temperature changes during the electromagnetic exposure. These changes are recorded as a sequence of temperature distribution images. The temperature evolution has been measured by taking a thermographic image every 20 s during microwave exposure and the immediately following phase.

III. EXPERIMENTS DESCRIPTION

We paid a particular attention to the analysis of the human head, as this is the body part mainly exposed, in normal conditions of mobile phone use. The exposed subjects have been a young man and woman in perfect health conditions. The main dimensions of the male head are shown in Fig. 1 and the main areas are summarized in Table I. Before starting any experiment, the subject was in the foreseen location, far from any electromagnetic and heat source, for at least 60 min.The head surface temperature, in different phases and experimental conditions, has been measured with a forward looking infrared (FLIR) camera (Thermovision model 570 by Agema, Bothell, WA) and two digital thermometers (MT100KC). The IR camera measures and images the emitted IR radiation from an object, through a pattern of 10 000 thermocouples located in the lens. The fact that radiation is a function of the surface temperature makes it possible for the camera to calculate and display this temperature. The radiation measured by the camera, however, does not only depend on the object temperature, it is also a function of the emissivity. It originates as well from the surroundings and is reflected by the object. Furthermore, the radiation from the object and the reflected radiation are also influenced by the absorption of the atmosphere (Fig. 2). Therefore, to measure the temperature accurately, it is necessary to compensate for the effects of a number of different radiation sources. Furthermore, the following parameters have been accurately determined prior to starting the measurements: emissivity, ambient temperature, atmospheric temperature, relative humidity of the air, and distance.

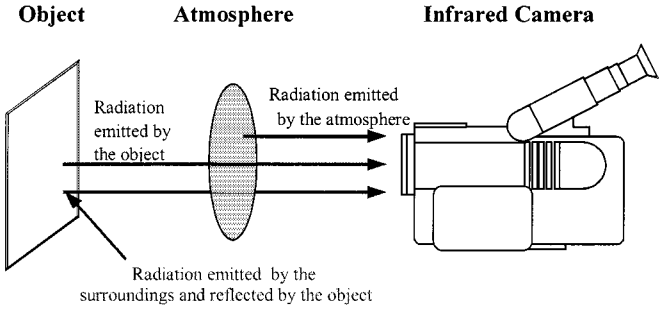

Fig. 2. Radiation contributions to general experimental setup.

A. Calibration

The most important parameter is the emissivity, defined as the ratio of the radiation flux per unit area emitted by the source to that of a black-body radiator at the same temperature in the same conditions. In short, it measures how much radiation is emitted by the object compared to that emitted by a perfect black body [12]. Normally, emissivities range from approximately 0.1 to 0.95. The human skin exhibits an emissivity close to 1.0.

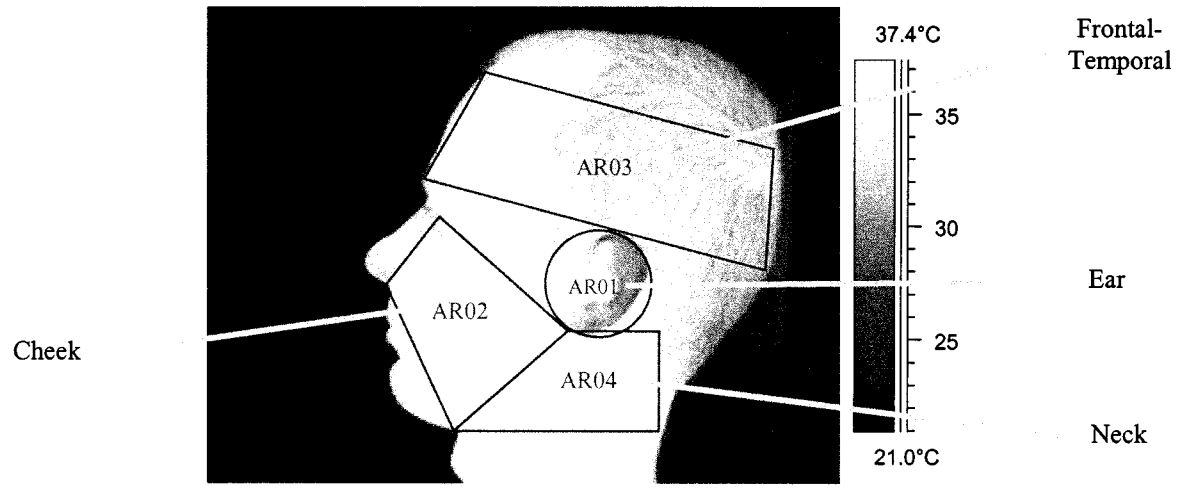

(a)

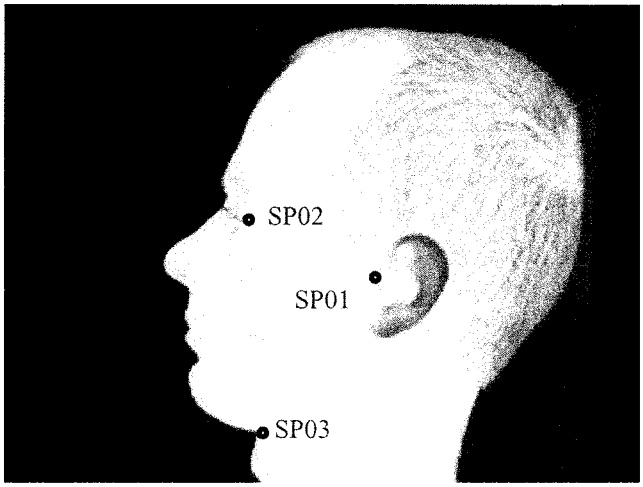

(b)

Fig. 3. Thermographic images. (a) Thermal analysis head areas. (b) Spots used for IR camera calibration.

At the beginning of each set of measurements, the temperature indicated by the IR camera has been calibrated in three points of the image [see Fig. 3(b)], using the data read by the digital thermometers, calibrated by the manufacturer using a calibration check equipment. The IR camera calibration has been performed in the following way.

A reference point is selected. Its temperature is measured using the digital thermometer thermocouple. The emissivity is altered until the temperature calculated by the IR camera agrees with the thermocouple reading. This is the emissivity value of the reference object. The temperature of the reference object must, however, not be too close to the ambient temperature for this to work. The resulting emissivity of the subject head skin was determined as having the value 0.98.

B. Measurement Criteria and Parameters Setup

In order to examine the surface thermal effects in the most detailed and reliable way, we have divided the subject head (profile section) in four different areas [see Table I and Fig. 3(a)]. We analyze the areas that are on the side of the mobile phone (subject left-hand side). For each experiment, we have investigated the surface temperature evolution over time, in the following two main phases, subsequent to the GSM mobile phone turned on: 1) *talking phase* (GSM mobile phone ON), corresponding to actual vocal conversation and 2) *switching off phase* (GSM mobile phone OFF), subsequent to the previous one.

Therefore, each measurement cycle is composed of these two phases. First measurements of the electromagnetic power density, using a radiation hazard meter (RAHAM), have shown that: 1) in *standby phase* (the mobile phone is turned on, but no call is ongoing), the electromagnetic power density is less than 1% of the *talking phase* one and 2) in *ringing phase* (the network requires the mobile phone to answer a call), the average electromagnetic power density is 10%–30% lower than the *talking* phase one. Moreover if the mobile phone is located far away from the human body, the duration of this phase can reach the maximum permitted by the network operator (3 min), but because of the distance, the thermal effects are negligible. If the mobile phone is close to the person, he or she normally answers within 1 min, thus, the duration of the *ringing phase* is limited compared to the

TABLE II
IR CAMERA EXPERIMENTS—PARAMETERS AND CHARACTERISTICS

Exp.	subject	case and location	phone model	signal reception level	talking duration	emissivity	ambient temperature	relative humidity	distance [cm]
I	young man	normal case, 4th floor	A	100%	15 min	0,98	20 °C	71%	80
II	young man	critical case, basement	A	40%	15 min	0,98	20 °C	73%	80
III	young man	normal case, 4th floor	A	100%	20 min	0,98	21 °C	77%	100
IV	young man	critical case, basement	A	80%	20 min	0,98	20 °C	71%	80
V	young man	normal case, 4th floor	B	100%	20 min	0,98	20 °C	71%	80
VI	young man	critical case, basement	B	90%	20 min	0,98	20 °C	71%	80
VII	young man	normal case, 4th floor	C	100%	20 min.	0,98	20 °C	71%	80
VIII	young man	critical case, basement	C	90%	20 min.	0,98	20 °C	71%	80
IX	young woman	normal case, 4th floor	A	100%	10 min.	0,98	20 °C	70%	50
X	young woman	critical case, basement	A	80%	20 min.	0,98	20 °C	70%	200

talking one. We have focused our analysis on the *average* surface temperature over each of the four areas. Using areas instead of spots or lines minimizes the measurement errors due to identification and positioning, and permits to follow temperature trend over time with higher accuracy.

Three types of GSM mobile phones have been used separately. They are models commercially available and commonly used, all three operating at 900 MHz and connected to a European GSM network operator. The three phones are called A, B, and C, respectively, with no reference to the commercial model. They are made by three different manufactures from Europe, U.S., and Japan, respectively. All the measurements have been performed at different levels (basement and fourth floor) of a building, located about 350 m away from the GSM base-station (BS) antenna, which the mobile phones were connected with. Both locations are far from other EMF sources and showed stable environmental conditions of temperature and humidity.

In order to evaluate and study the surface temperature trend, two types of experimental situations have been examined as follows. 1) *Ordinary cases*: favorable reception–transmission conditions. *Location*: fourth floor (12 m above ground level). 2) *Critical cases*: extreme situations, unfavorable reception–transmission conditions. *Location*: basement (4 m below ground level). Every measurement has been made in both of the different cases.

The parameters and characteristics of every performed experiments are detailed in Table II, where the specified distance is between the subject ear of the side shown to the camera and the Thermovision camera. The distance between the mobile phone ear-piece and the subject ear, in *talking phase*, was approximately 0.5 cm in experiments I–VIII. They were never in touch to exclude all the phenomena related to local pressure and friction by the mobile phone on the human ear, potentially inducing a local temperature increase perturbing the heating effect due to electromagnetic waves. In experiments IX–X, however, the phone ear-piece and subject ear have been placed in soft touch (as in the most common mobile phone use) in order to determine the influence of the local pressure and friction between the phone and ear on the temperature variation.

On the other hand, it is interesting to emphasize that we have noted that the presence of the mobile phone close to the head, and the reduction in ventilation of head surfaces are not significantly contributing to the temperature increase. The influence on head temperature increase due to heat radiation induced by the mobile phone electronic parts is under study.

IV. SURFACE TEMPERATURE VARIATION OF HEAD AREAS

In Sections V and VI, diagrams represent the average surface temperature variation over time for any head area of each experiment described in Table I. The experimental data have been interpolated by trend lines. In order to highlight the average surface temperature trend of different human head areas, the following best-fit trend lines have been used: 1) a line showing the temperature trend over time in the *talking* phase: linear for the

ear area, quadratic for all the other areas and 2) a line showing the temperature trend over time in the *switching off* phase: cubic for all the areas.

The average surface temperature trends have been thoroughly analyzed, with the purpose of extrapolating all the common aspects characterizing the various experiments. In particular, sensitivity analyses have been performed, using the following four criteria:

1) head areas exposed to radio waves;
2) mobile phone types;
3) experiment duration;
4) experiment location.

The main attention has been paid to the *relative temperature*, i.e., the trend over time, rather than the absolute temperature values. These are indeed very much depending on specific experiment date, time, location, external parameters (room temperature, humidity, etc.), and subject physiological status.

V. Ear-Area Analysis

In all the experiments, the $T_{s\ \mathrm{avg}}$ (average surface temperature) trend of the human *ear* area is similar (Fig. 4). During the *talking* phase, the $T_{s\ \mathrm{avg}}$ trend is increasing and can be approximated well by a linear curve. The temperature rise is occurring continuously through all the *talking phase* period. It ends immediately when the phone switches off. The temperature increase range varies between minimum 1 °C (experiment I) and 2.4 °C (experiment II).

A. Sensitivity to Type of Mobile Phone

The measured $T_{s\ \mathrm{avg}}$ increase is not the same for the three different phones, all other conditions (area, location, duration) being equal. In particular, the maximal $T_{s\ \mathrm{avg}}$, measured at the end of *talking phase* (basement, 20-min exposure), has been higher for phone B (1.8 °C), intermediate for phone C (1.5 °C), and lower for phone A (1.1 °C). Hence, different mobile phones induce different thermal effects on the head.

B. Sensitivity to Location

The sensitivity to location is actually a sensitivity to the level of signal received by the phone. We have found that, at fourth floor, the signal level has always been 100%, while in the basement, it has been varying between 40%–80% of the phone maximum level. Hence, the measured $T_{s\ \mathrm{avg}}$ increase is not same for the two locations, all other conditions (area, mobile phone type, duration) equal. In particular, the relative $T_{s\ \mathrm{avg}}$ increase, measured across the *talking phase* (15-min exposure, phone A), was higher in the location where the signal level is lower (basement). As a matter of fact, analyzing experiments I and II, the temperature increase rate in the *talking phase* is faster in the basement (signal level 40%) than at fourth floor (signal level 100%), as shown in Fig. 4(a): the slope is different. On the other hand, the measured $T_{s\ \mathrm{avg}}$ increase is very similar for the two locations, all other conditions (area, mobile phone type, duration) equal, if the signal level is similar.

C. Sensitivity to Exposure Duration

The measured $T_{s\ \mathrm{avg}}$ at the end of the *talking phase* is not the same for the different time exposures, at other conditions (area, location, mobile phone type) equal, while the increase rate is the same. In particular, the relative $T_{s\ \mathrm{avg}}$ increase, measured across the *talking phase* (phone A, fourth floor), was higher for an exposure duration of 20 min (1.4 °C) than for an exposure duration of 15 min (1.2 °C). Analyzing experiments I and III, the different peak temperature can be seen in Fig. 4(b).

This means that a longer exposure induces a higher thermal effect.

D. Sensitivity to Contact Between Mobile Phone and Human Ear

While the distance between the phone ear-piece and subject ear, in *talking phase*, has been $\cong$ 0.5 cm in experiments I–VIII, the two parts have been placed in soft touch in experiments IX–X in order to determine the influence on temperature variation induced by local pressure and friction between the mobile phone and human ear (Fig. 5). The measured $T_{s\ \mathrm{avg}}$ increase is not the same for the two situations, all other conditions (area, location, mobile phone type, duration) equal. In particular, the relative $T_{s\ \mathrm{avg}}$ increase, measured across the *talking phase* (phone A, ear area, basement, 20 min), has been significantly higher in *soft-touch* conditions (2.8 °C) than in no-touch conditions (1.2 °C). Analyzing experiments IV and X, the different temperature increase rate can be seen in Fig. 5. The increase can be attributed to phenomena related to local pressure and friction by the phone on the ear, which induces a significant local temperature increase in addition to microwave heating. Hence, we can say that in soft touch conditions: 1) about 40%–45% of total ear heating is due to microwave heating and 2) about 55%–60% of total ear heating is due to pressure and friction.

E. Switching Off Phase Analysis

Immediately after switching off the mobile phone, the ear $T_{s\ \mathrm{avg}}$ starts decreasing. In some cases, the temperature decrease is sharper, to the extent that temperature reaches lower levels than the initial experiment temperature (negative overshooting) due to thermal inertia. After an oscillation cycle, the temperature gradually goes back to the initial experiment level. In these cases, the head temperature trend is similar to a second-order system response to a step with dump. The measured $T_{s\ \mathrm{avg}}$ decrease trend is different for different absolute peak temperatures, all other conditions (area, location, duration, mobile phone type) equal. In particular, the relative $T_{s\ \mathrm{avg}}$ decrease, measured after the end of the *talking phase* (phone A, 20 min), was higher in the basement (peak temperature 35.3 °C) than at fourth floor (peak temperature 34.7 °C).

VI. Cheek, Frontal–Temporal, and Neck Areas Analysis

In all the performed experiments, the $T_{s\ \mathrm{avg}}$ absolute trends of the other three analyzed head areas (cheek, frontal temporal, and neck areas) are quite different from the ear area $T_{s\ \mathrm{avg}}$. For the two areas of cheek and neck, we note that during *talking*

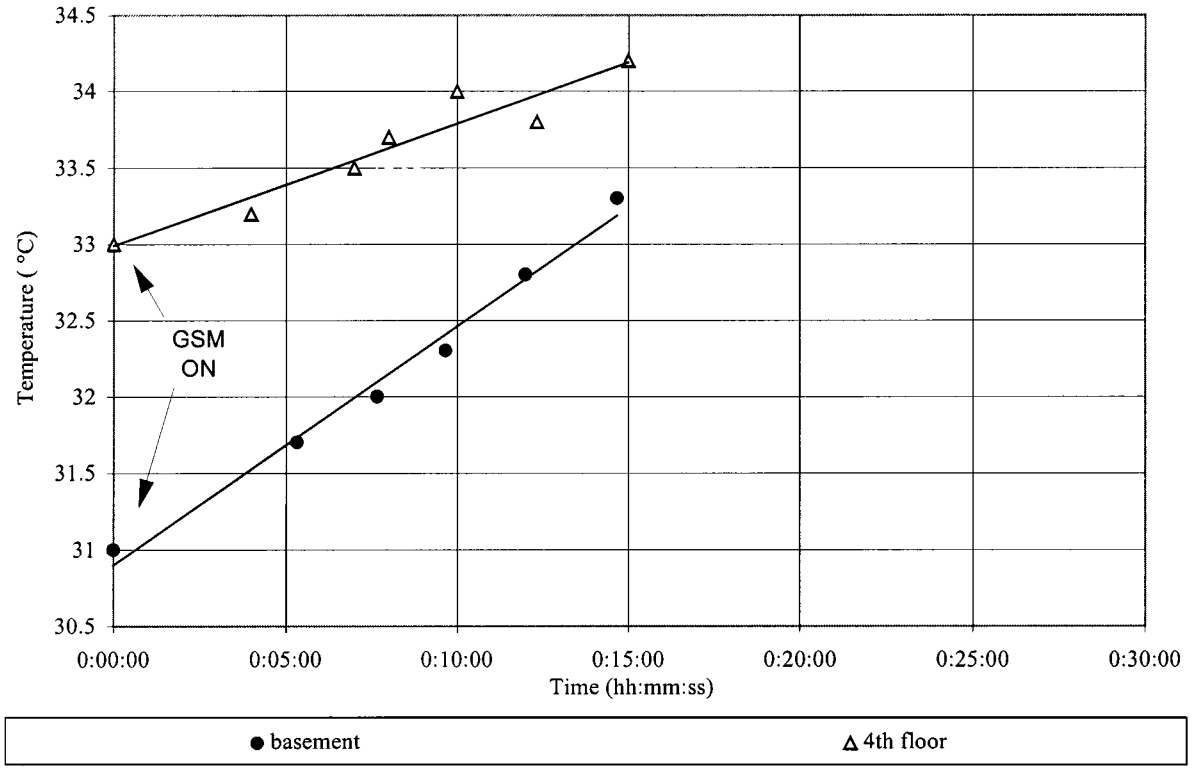

(a)

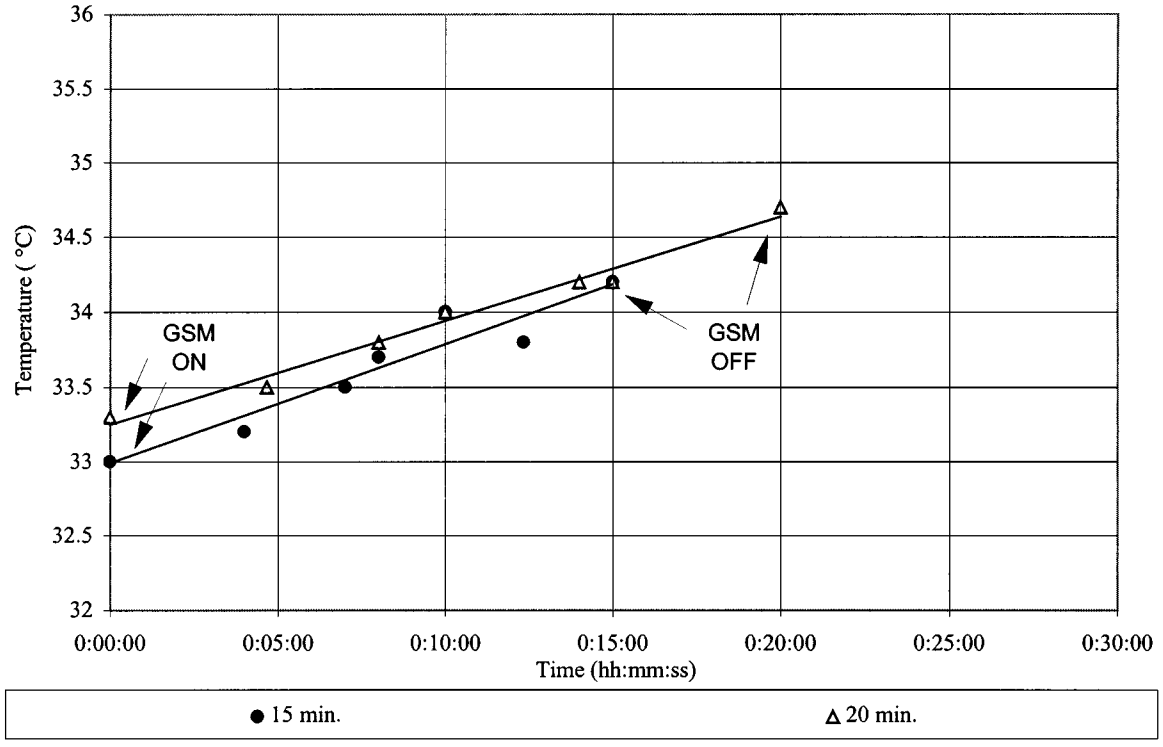

(b)

Fig. 4. Temperature trend of human ear lobe area, exposed to 900 MHz (phone A). (a) Comparison between average temperature measured in basement and fourth floor during 15-min talking phase. (b) Comparison between average temperature measured during 15- and 20-min talking phases at fourth floor.

phase, the $T_{s\,\mathrm{avg}}$ trend follows a similar trend in all the experiments. The $T_{s\,\mathrm{avg}}$ is gradually increasing in the exposure for the first 5–7 min. The temperature increase after 7-min exposure was between 0.3 °C (experiment I) and 1.1 °C (experiment VI) for the cheek, and between 0.3 °C (experiment I) and 0.8 °C (experiment IV) for the neck (Fig. 6). During the following 5 min,

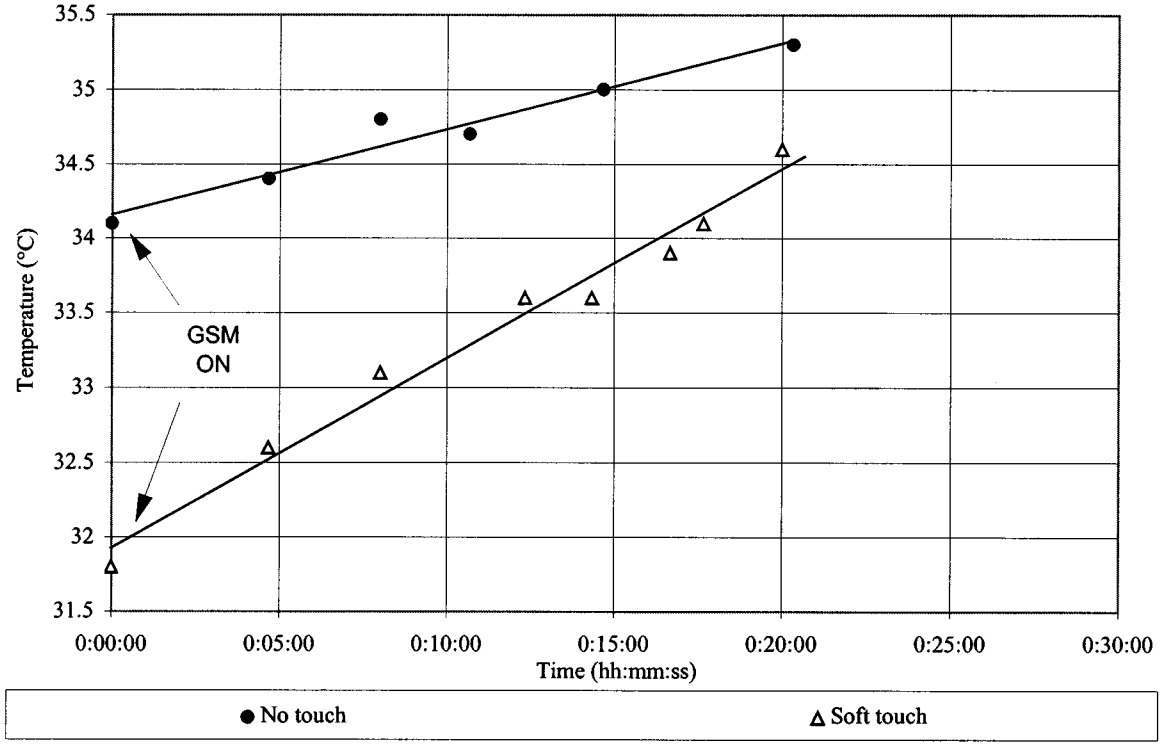

Fig. 5. Temperature trend of human ear-lobe area, exposed to 900 MHz (phone A), comparison between average temperature, measured with mobile phone in soft touch and not at all in touch with the ear, during 20-min talking phase, in basement.

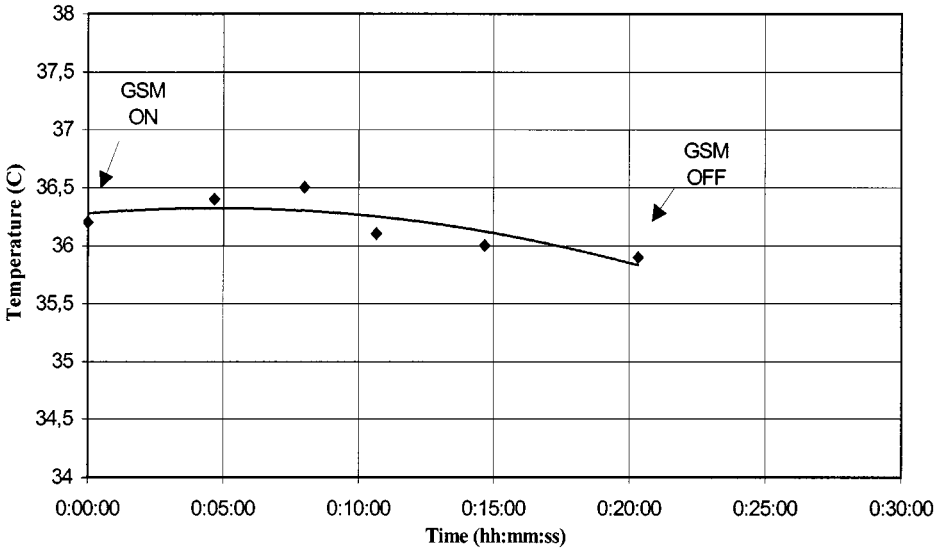

Fig. 6. Temperature trend of human neck area, exposed to 900 MHz (phone A); average temperature measured in basement during 20-min *talking*.

the temperature gradually decreases by 0.3 °C–0.5 °C versus the peak level reached after around 7 min.

Concerning the frontal–temporal area, we noted that the $T_{s\ \mathrm{avg}}$ trend is normally constant or slightly decreasing. Only with the lowest reception signal level (experiment II), the frontal–temporal area has shown a slight temperature increase. In general, the frontal–temporal temperature is qualitatively following a trend similar to the ear, with a much lower slope (around 1.6 °C–1.9 °C/20 min less than the ear). This leads, in the cases when the ear temperature trend has shown a slight increase, to observe a temperature decrease on the frontal-temporal area.

The physical reason for this behavior is that the temperature rise in the ear leads to a temperature compensation in the surrounding tissues provided by *termoregulatory processes* of the body. The maintenance of a certain temperature is of vital importance to the organism because of all biological processes are conditioned by temperature. In the presence of thermal environmental and internal stresses, the body temperature first increases and then decreases following the onset of a thermoregulatory

TABLE III
MEASUREMENTS ERRORS. (a) DUE TO AREA IDENTIFICATION. (b) DUE TO PARAMETER SETTING

Area nr.	Area	Error
AR01	Ear	$< \pm 0.05$ °C
AR02	Cheek	± 0.05 °C
AR03	Frontal-Temporal	± 0.05 °C
AR04	Neck	$< \pm 0.05$ °C

(a)

Parameter	Parameter error	Temperature error
emissivity	± 0.005	± 0.05 °C
ambient temperature	± 2.5 °C	± 0.05 °C
relative humidity	± 10 %	± 0.00 °C
distance	± 5 cm	± 0.00 °C
Total		± 0.1 °C

(b)

response mediated by the endocrine and cardiovascular systems [13]. The mechanisms of heat regulation are activated in several ways and the thermal receptors in the skin play a key role. In this case, the surrounding tissues (cheek, frontal-temporal area, neck) react to a local heating of the ear trying to compensate it via heat losses, leading to a local temperature decrease or at least a lower increase. In the cases where the ear temperature significantly increases, the temperature slightly increases also on the surrounding areas, as the heating rate is faster than the body thermoregulation response capability.

It is interesting to highlight that the obtained results are in accordance with the averaging time used in the microwave safety standards [14]. In fact, the exposure standards are based on thermal considerations and a thermal time constant averaging time of 6 min has been recommended.

VII. ERROR ANALYSIS

The experimental data are affected by the following identified measurement errors.

A. Area Identification (Size and Position)

There are errors due to: 1) subject head micromovements during the whole experimental duration and 2) graphical area drawing by IR camera image analysis software. These errors have been evaluated as indicated in Table III(a). They have been determined by verifying the area average temperature change, for an area positioning error of ± 0.3 cm and an area size error of ± 0.6 cm^2.

B. Instrument Accuracy

According to the manufacturer (Agema-Flir, Bothell, WA), the IR video camera used to measure the head surface temperature has an accuracy of ± 0.05 °C (difference between indicated and actual temperature). On the other hand, it is worth mentioning that the instrument sensitivity is 0.1 °C (minimum detectable temperature). Analyzing the head with no GSM present over a 20-min duration, we have not been able to detect any temperature variation in any area, and we have considered the temperature noise to be within the instrument accuracy.

C. Boundary Parameters Accuracy

The measured temperature is affected by a series of boundary parameters settings, according to Section III. The errors induced by each of these parameters on the final area average temperature are summarized in Table III(b). They have been determined by verifying the area average temperature change for the relative parameter setting change. The parameter error corresponds to the error of the instrument augmented by the instrument reading error (thermometer, barometer, meter). The overall maximum temperature error is about 0.2 °C for all areas.

VIII. LINK BETWEEN SURFACE AND INNER TEMPERATURE

The experiments have permitted to establish the surface temperature. Hence, it is important to find a consistent link between surface and inner temperatures. Before doing so, a few concepts regarding heat transmission need to be recalled.

In conventional heating systems, heat is transmitted to the surface of a medium by conduction, convection, or radiation. On the other hand, the phenomena occurring in organic tissues exposed to microwave heating are different: heat is generated inside of the medium by dielectric heating. It is a volume effect, inducing a temperature increase much faster than a conventional heating system [15].

Microwave heating can be modeled using the bioheat equation. In order to establish the link between the surface temperature and the inner one, we have preferred to perform not a numerical, but an experimental analysis. The heat equation numerical solution indeed inside the human head is a rather complicated problem, not necessarily solvable, because of the difficulty of establishing adequate thermal boundary conditions inside of the head. The problem is quite complex for inhomogeneous materials (different media separated by interfaces), anisotropic materials (permittivity a function of direction), and when permittivity varies significantly with temperature. The human body has a complex surface and internal geometry, and is composed of tissue with spatially varying dielectric properties.

Our choice, therefore, has been to perform an experimental analysis using the IR camera. We have examined different nonliving tissues of young beef meat, exposed to the microwave radiation emitted by phone A, in two different operating conditions. The parameters and characteristics of each of the performed experiments are detailed in Table IV. We have assumed that the temperature trend inside of the beef meat tissue could be used like a "maximum reference level" for approximating that inside of the human head. As a matter of fact, the intensity-based heating effect of microwave radiation is independent of whether the irradiated organism is alive or dead. The "active thermoregulation" (heat-transfer mechanisms by employing internal circulating fluids), characteristic of living organisms, is excluded in this experiment. Thus, are necessarily excluded all the effects contingent to the aliveness of the organism, such as, in particular: metabolic heat production, local tissue blood

TABLE IV
INNER TEMPERATURE EXPERIMENTS—PARAMETERS AND CHARACTERISTICS

Exp.	subject	case and location	mobile phone type	signal reception level	exposure duration	emissivity	ambient temperature	relative humidity
I	beef meat	normal case , 4th floor	A	100%	20 min.	0,98	21 °C	71%
II	beef meat	critical case, basement	A	50%	20 min.	0,98	20 °C	71%

flow, and cutaneous vasodilation. On the other hand, the "passive thermoregulation" (heat transfer mechanisms via radiation, conduction, convection) is intact.

We have performed the experiment, putting a piece of beef meat, about 28-mm thick, onto a wooden support with an intermediate isolating rubber sheet. No electromagnetic source has been left within 20 m from the experimental location. After leaving the meat in these conditions for more than 60 min, it has about reached the room temperature at its surface (18.5 °C). We have then put phone A onto the free meat surface and switched it on in *talking phase*. We have photographed the temperature trend within the beef meat section every 5 min starting from mobile phone switch on. The plot of the temperature trend versus the meat thickness d, every 5 min (from 0 to 20 min), has been recorded. The measurement was taken along an axis perpendicular to the surface in touch with the phone, starting from the surface itself. The overall temperature, not perfectly constant at start up, first becomes uniform inside the meat, and then starts increasing at a higher rate on the superficial layers and at a lower rate in the inner layers.

Considering only the temperature trend inside the meat at the beginning and at the end ($t = 20$ min), we have interpolated both series of experimental data with best-fit quadratic trend-lines [see Fig. 7(a)]. The result clearly shows that the temperature increase at the surface is higher than in inner layers. As an example, for a surface temperature increase of 1.6 °C, there is a temperature increase of 0.3 °C at 25 mm from the surface.

Fig. 7(b) shows the trend within the meat thickness d of the difference between the temperature after 20-min *talking* and the initial temperature

$$\Delta T(d) = T_{\text{trendline}}(d,\ 20\ \text{min}) - T_{\text{trendline}}(d, 0). \quad (1)$$

Due to our quadratic interpolation of temperature at 0 and 20 min, the ΔT has a quadratic trend versus tissue thickness d as well. It can be observed that the variation is similar to an exponential with a skin depth of about 15 mm, which is indeed the value valid for a human body at 900 MHz.

IX. CONCLUSIONS

The purpose of this paper has been to experimentally determine the temperature trend of an actual human head, exposed to microwaves emitted by GSM mobile phones at 900 MHz. These fields are known to penetrate exposed tissues and produce heating due to energy absorption. Even very low levels of RF energy produce a small amount of heat. Although the mobile telephone handsets transmit much less power (2-W maximum) than a BS (e.g., 10-W maximum, to be augmented by the antenna gain), the user's body absorbs significantly more power from the handset antenna, and the head of the user receives the highest localized RF exposure because of the short distance.

We have divided the subject head in four different areas and investigated the surface temperature evolution over time in the following two main phases: 1) *talking phase* (phone ON) and 2) *switching off phase* (phone OFF), subsequent to the previous one.

We have also verified that emission during *standby* phase is not thermally relevant. The experiments give a complete picture of the surface temperature distributions in the human head profile, using different mobile phones and operating at different signal-level conditions. We have directly measured the surface temperature, and indirectly determined the corresponding inner temperature.

The results are as follows.

1) The most significant surface temperature increase occurs:
   a) on the ear lobe;
   b) at the end of *talking phase*;
   c) for higher duration (20 min);
   d) at lower signal conditions (50% of the maximum, in a basement).
2) In the ear lobe region, after 15- and 20-min *talking* time, surface temperature increases varies from 1.0 to 2.4 $\pm$0.2 °C, depending on location (signal level) and phone type.
3) In the regions surrounding the ear, such as the cheek and neck, during the *talking phase*, the surface temperature first increases and then decreases because of thermoregulation effects.
4) With reference to beef meat heating, it is possible to deduce that to a surface temperature increase of 1.6 °C corresponds an inner temperature increase of 0.75 °C at 10 mm from the surface, and 0.3 °C at 25 mm from the surface.
5) We have directly measured the total body temperature and we note that it does not significantly change during and after any of the experiments.

Those results should be compared with the *International Technical Standards* [16]–[18], according to which mobile telephones are made, which do not allow them to cause any significant heating. The head of the mobile phone user, in particular, the ear, receives the highest localized RF exposure. *This localized RF exposure should not cause any local temperature*

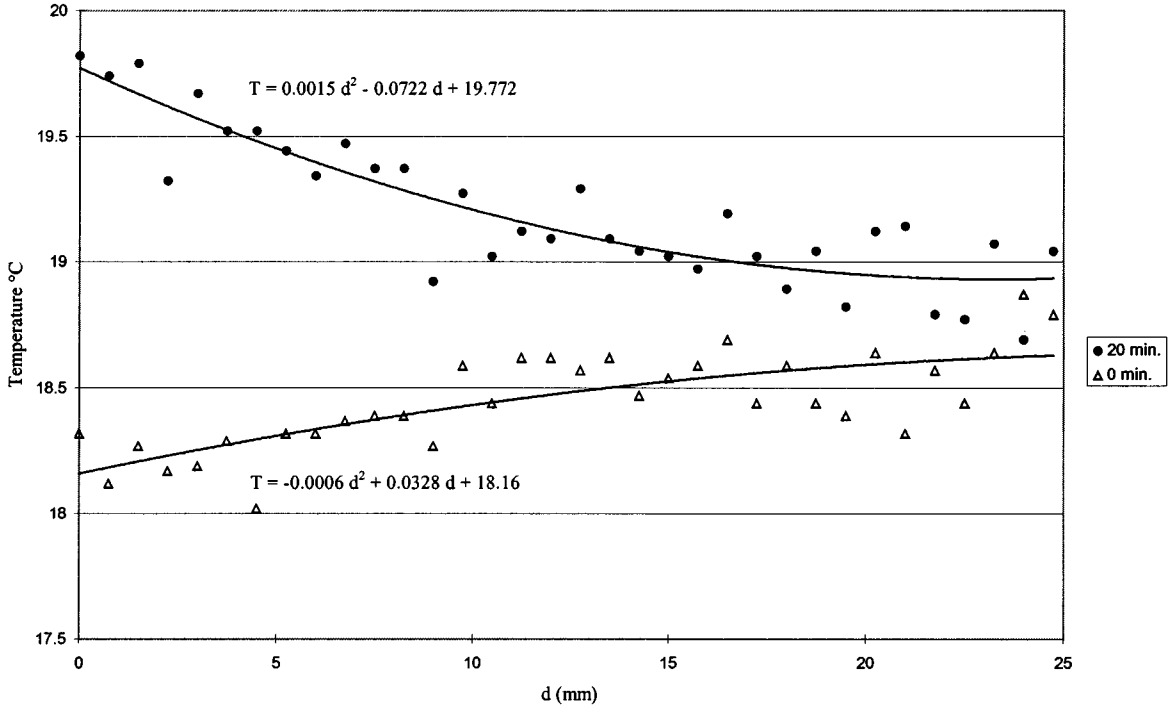

(a)

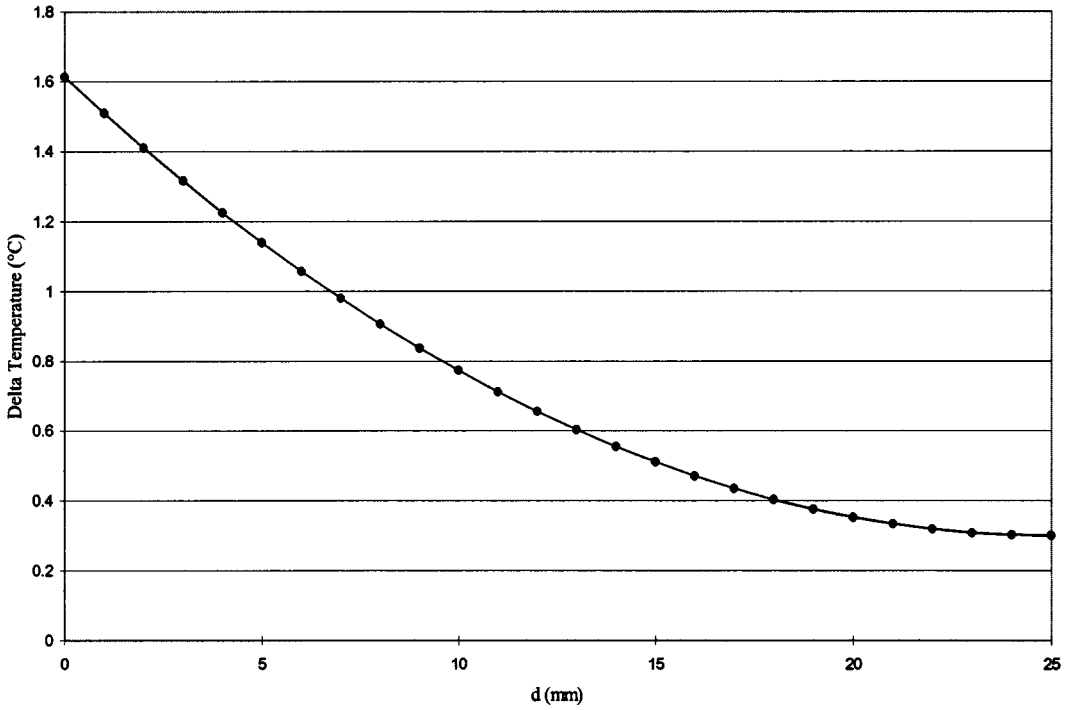

(b)

Fig. 7. Temperature trend inside meat. (a) At start ($t = 0$) and end ($t = 20$ min). (b) Difference between temperature trend after 20-min talking and at start as a function of penetration.

increases in excess of 1 °C [19]. However, our experimental data show that the average temperature increase on the ear lobe ranges from 1.0 to 2.4 ±0.2 °C.

ACKNOWLEDGMENT

The authors would like to thank the reviewers of this paper's manuscripts for their useful suggestions and remarks.

REFERENCES

[1] A. Vander Vorst and F. Duhamel, "Mobile telephony recommendations vs. biology," in *Proc. Int. Telecommun. Conf.*, vol. III, June 1998, pp. 356–360.

[2] A. Vander Vorst, "What about safety when using mobile telephony," in *Proc. Microcoll '99*, Mar., pp. 35–39.

[3] P. R. Riu, K. R. Foster, D. W. Blinck, and E. R. Adler, "A thermal model for humans thresholds of microwave-evoked warmth sensations," *Bioelectromag.*, vol. 18, pp. 578–583, 1997.

[4] N. Kuster and Q. Balzano, "Energy absorption mechanism by biological bodies in the near field of dipole antennas above 300 MHz," *IEEE Trans. Veh. Technol.*, vol. 41, pp. 17–23, Jan. 1992.
[5] C. Polk and E. Postow, *Handbook of Biological Effects of Electromagnetic Fields*. Boca Raton, FL: CRC Press, 1996, pp. 314–322.
[6] M. D. Taurisano, "Biological effects of electromagnetic waves due to GSM mobile phones," Elect. Eng. thesis, Dept. Elect. Eng., Univ. catholique de Louvain, Louvain-la-Neuve, Belgium, 1999.
[7] M. D. Taurisano and A. Vander Vorst, "Measurements of thermal effects induced on a human head exposed to 900 MHz mobile phone," in *IEEE MTT-S Int. Microwave Symp. Dig.*, Boston, MA, June 2000.
[8] M. Anbar, "Quantitative and dynamic telethermometry—A fresh look at a critical thermology," *IEEE Eng. Med. Biol.*, vol. 14, pp. 15–16, Jan./Feb. 1995.
[9] Y. V. Gulyaev, A. G. Marcov, L. G. Koreneva, and P. V. Zakharov, "Dynamical infrared thermograpy in humans," *IEEE Eng. Med. Biol.*, vol. 14, pp. 766–771, Nov./Dec. 1995.
[10] A. W. Guy, "Analyses of electromagnetic fields induced in biological tissues by thermographic studies on equivalent phantom," *IEEE Trans. Microwave Theory Tech.*, vol. MTT-19, pp. 205–214, Feb. 1971.
[11] C. U. Hochuli and G. Kantor, "An analysis of minimally perturbing temperature probe and thermographic measurements in microwaves diathermy," *IEEE Trans. Microwave Theory Tech.*, vol. MTT-29, pp. 1285–1291, Dec. 1981.
[12] T. C. Cetas, "Practical thermometry with a thermographic camera: Calibration, transmittance, and emittance measurements," *Rev. Sci. Instrum.*, vol. 49, pp. 245–254, Feb. 1978.
[13] S. M. Michaelson, "Biological effects and health hazards of RF and MW energy: Fundamentals and overall phenomenology," in *Biological Effects and Dosimetry of Nonionizing Radiation*, M. Grandolfo, S. M. Michaelson, and A. Rindi, Eds. New York: Plenum, 1983, pp. 337–357.
[14] K. R. Foster, A. Lozano-Nieto, P. J. Riu, and T. S. Ely, "Heating of tissues by microwaves: A model analysis," *Bioelectromag.*, vol. 19, pp. 420–428, 1998.
[15] J. Thuery, *Microwaves: Industrial Scientific and Medical Applications*. Norwood, MA: Artech House, 1992.
[16] "Restrictions on human exposure to static and time varying electromagnetic fields and radiation," Nat. Radiolog. Protection Board, NRPB document, vol. 4, 1993.
[17] International Commission on Non-Ionizing Radiation Protection, "Guidelines for limiting exposure to time-varying electrical, magnetic, and electromagnetic fields (up to 300 GHz)," *Health Phys.*, vol. 74, pp. 494–522, Apr. 1998.
[18] "Considerations for human exposure to emf's from mobile telecommunication equipment (MTE) in the frequency range 30 MHz—6 GHz," European Committee Electrotech. Standardization, European Specification CENELEC, Feb. 1997.
[19] "Electromagnetic Fields and public health: mobile phones and their base stations," World Health Organization, Geneva, Switzerland, Fact Sheet 193, May 1998.

Maria Daria Taurisano received the Electronic Engineering degree from the Politecnico di Torino, Turin, Italy, in 1999, and is currently working toward the Ph.D. degree in electronic engineering at Université catholique de Louvain (UCL), Louvain-La-Neuve, Belgium.

She is currently with the Microwave Laboratory, UCL, where she is involved in research dealing with the biological effects of EMFs generated by mobile phones on the humans. Her research interests include digital communications, biological effects of microwave exposure, electromagnetic dosimetry, and bioelectromagnetics.

André Vander Vorst (M'64–SM'68–F'86) was born in Brussels, Belgium, in 1935. He received the Electrical and Mechanical Engineer degrees and the Ph.D. degree in applied sciences from the Université catholique de Louvain (UCL), Louvain-la-Neuve, Belgium, in 1958 and 1965, respectively, and the M.Sc. degree in electrical engineering from the Massachusetts Institute of Technology (MIT), Cambridge, in 1965.

From 1958 to 1964, he was involved with fast switching of magnetic cores. From 1964 to 1966, he worked under a NATO Fellowship, first at MIT, then at Stanford University, both in the field of radio-astronomy. In 1966, he founded the Microwave Laboratory, UCL, which he is currently heading, beginning with research on loaded waveguides and cavities. The laboratory is currently conducting research on atmospheric transmission and diffraction up to 300 GHz, the methodology of designing and measuring active and passive circuits up to 100 GHz, and microwave bioelectromagnetics, namely, the transmission between the peripheral and central nervous systems, using microwave acupuncture as a stimulus. While with UCL, he has been Head of the Electrical Engineering Department (1970–1972), Dean of Engineering (1972–1975), Vice-President of the Academic council of the University (1973–1975), President of the Open School in Economic and Social Politics (1973–1987). He is currently associated with the UCL, where he became an Assistant (1958), Assistant Professor (1962), Associate Professor (1968), and Professor (1972). He has authored or co-authored three textbooks, several chapters, and a variety of scientific and technical papers in international journals and proceedings.

Dr. Vander Vorst is a member of the National Committee of the URSI and of various committees on communications, microwaves, and education. He has been active in IEEE Region 8, as well as in the European Microwave Conferences. He is also a member of Academica Europaea and The Electromagnetics Academy. He was the 1986 recipient of the Sitel Prize and the 1994 IEEE Microwave Theory and Techniques Society (IEEE MTT-S) Meritorious Service Award.